Transfer Learning for Spatial Autoregressive Models with Application to U.S. Presidential Election Prediction

Hao Zeng[1], Wei Zhong[2] and Xingbai Xu[2]

[1]Department of Statistics and Data Science

Southern University of Science and Technology

[2]MOE Key Lab of Econometrics

WISE and Department of Statistics and Data Science in SOE

Paula and Gregory Chow Institute for Studies in Economics

Xiamen University

September 10, 2024

Abstract

It is important to incorporate spatial geographic information into U.S. presidential election analysis, especially for swing states. The state-level analysis also faces significant challenges of limited spatial data availability. To address the challenges of spatial dependence and small sample sizes in predicting U.S. presidential election results using spatially dependent data, we propose a novel transfer learning framework within the SAR model, called as tranSAR. Classical SAR model estimation often loses accuracy with small target data samples. Our framework enhances estimation and prediction by leveraging information from similar source data. We introduce a two-stage algorithm, consisting of a transferring stage and a debiasing stage, to estimate parameters and establish theoretical convergence rates for the estimators. Additionally, if the informative source data are unknown, we propose a transferable source detection algorithm using spatial residual bootstrap to maintain spatial dependence and derive its detection consistency. Simulation studies show our algorithm substantially improves the classical two-stage least squares estimator. We demonstrate our method's effectiveness in predicting outcomes in U.S. presidential swing states, where it outperforms traditional methods. In addition, our tranSAR model predicts that the Democratic party will win the 2024 U.S. presidential election.

Keywords: Spatial autoregressive model, transfer learning, U.S. presidential election, spatial data analysis, high dimensional analysis.

1 Introduction

In recent years, amounts of Geographic Information Science (GIS) data have been used in election campaigns (Peters et al., 2004). Geography is the common denominator of where voters live, how residents engage in the voting process, how officials manage elections, and where elections campaign runs. Based on population data and geographic information, election district boundaries are resettled to draft multiple proposed plans and demonstrate the effects of several approaches. Political campaigns make full use of geographic information and related tools to obtain underlying support from voters, especially the ones from swing states, which are pivotal in determining the outcome of elections. Swing states, also known as battleground states, are crucial because they do not consistently support one party, making their election outcomes unpredictable and highly influential in election results. Shaping voter preference in swing states is an essential problem, especially for prediction. Including spatial information in data analysis brings a novel insight into the prediction. There are at least two challenges in using spatial information for predicting U.S. presidential elections: one is leveraging spatial information effectively to predict election outcomes with considering the impact of spatial factors, and the other is the limited data from swing states. Finding ways to use information from other states to analyze spatial factors and predict the final result is crucial to overcoming these challenges.

Spatial dependence among spatial units exists widely in various fields including economics (Anselin, 1988), finance (Grennan, 2019), political science (Peters et al., 2004), ecology (Ver Hoef et al., 2018) and climate sciences (Okunlola et al., 2021) and so on. The spatial autoregressive (SAR) model (Cliff and Ord, 1973; Ord, 1975; Cliff and Ord, 1975) and its variants are extensively applied in numerous empirical studies concerning spatial competition and spatial spillover effects. For instance, the SAR model is employed to investigate the crime rates in 49 areas of Columbus, Ohio (Anselin, 1988), budget spillover effects and policy interdependence (Case et al., 1993),

cigarette demands in various states in the U.S. (Baltagi and Li, 2004), agricultural land prices in Northern Ireland (Kostov, 2009), the mutual influence on the stock returns of companies with the same headquarters location (Pirinsky and Wang, 2006) and the group effect of the dividend policy of listed companies (Grennan, 2019).

When the sample size of the target data is limited, it is possible to obtain less precise estimates for most statistical models. This issue is particularly relevant in spatial econometrics, where sample sizes can often be quite limited. For instance, in the study investigating crime rates in Columbus, Ohio, the sample size is restricted to just 49 (Anselin, 1988). This limitation underscores the necessity for additional research aimed at leveraging information from similar datasets to elevate estimation performance. Consequently, there is a pressing need for the exploration of methods to improve the estimation performance of the SAR models through the incorporation of information derived from similar source datasets. Transfer learning is a useful approach to incorporate information from source datasets (Pan and Yang, 2009; Torrey and Shavlik, 2010; Zhuang et al., 2021; Hu and Zhang, 2023). The main idea of transfer learning is that the knowledge acquired in one context can be transferred to improve the performance of estimation or prediction when applied to another, even if the two tasks or domains are not identical. In transfer learning, there are typically two main components: (1) The first one is the *target domain*, to which the knowledge is transferred. The target domain is of our interest but particularly its sample size is limited. (2) The second one is the *source domain*, from which the knowledge is transferred. In general, the model is pre-trained using the source datasets.

In the recent literature, Bastani (2021) introduced a two-step estimator that employs high-dimensional techniques to capture biases between the target and source data and has provided an upper bound for the proposed estimators. Li et al. (2022b) considered transfer learning for estimation and prediction of a high dimensional linear regression and proposed a novel data-driven Trans-Lasso method for detecting the transferable sources. Tian and Feng (2023) introduced a

novel entropy-based method for identifying transferable sources and further constructed confidence intervals for each coefficient under the generalized linear model. For more reference on related works, see Cai and Pu (2019), Cai et al. (2024a,b), and Li et al. (2022c,a).

In this paper, in order to deal with two aforementioned challenges, spatial dependence and sample limitation, in U.S. presidential election prediction problems, we present a transfer learning framework within the SAR model, which we refer to as **tranSAR**, designed to improve both estimation and prediction. Our study makes three contributions from methodology, statistical theory and empirical application in the literature of the SAR models. First, in methodology, we introduce a two-stage algorithm ($\mathcal{A}$-TranSAR), consisting of a transferring stage and a debiasing stage, to estimate the unknown parameters when the informative source data indexed by $\mathcal{A}$ are known. If we do not know which sources to transfer, a transferable source detection algorithm is proposed to detect informative sources data based on spatial residual bootstrap to retain the spatial dependence. To the best of our knowledge, this is the first work to introduce the transfer learning to the SAR models. Second, in statistical theory, we establish the theoretical convergence rates for the $\mathcal{A}$-TranSAR estimators under the SAR model and theoretically show that the transfer learning can improve the estimation accuracy with the help of the information from the transferable source data. We also derive the detection consistency of the transferable source detection algorithm to avoid the negative transfer when which sources to transfer is unknown. Third, in the empirical application, we apply our method to predict the election outcomes in swing states in the U.S. presidential election via utilizing polling data from the last U.S. presidential election along with other demographic and geographical data. The empirical results show that our method outperforms traditional spatial econometrics methods.

Here, we emphasize the differences between our work and Tian and Feng (2023). Although our work shares a similar idea of transfer leaning with the previous literature, there are at least two significant differences from both theoretical and algorithmic perspectives. (1) Tian and Feng

4

(2023) is based on generalized linear models for independent data. In contrast, our research focuses on spatially dependent data, which brings significant challenges for theoretical guarantees. This is because previous theories heavily rely on concentration inequalities applicable to independent data, and few concentration inequalities have been established for spatially dependent data. To address this, we develop a new theoretical foundation tailored to spatially correlated data. (2) For the algorithmic aspect, the transferable detection method in Tian and Feng (2023) relies on sample splitting to identify transferable sources, a technique that is inapplicable for spatial data as spatial data are not independent. To this end, we propose a new method based on spatial bootstrap and establish its theoretical guarantees.

In the rest of our paper, we firstly introduce the real application problem (predicting the U.S. presidential election result) and the associated transfer learning framework for the SAR model in Section 2. Then, we introduce its estimation and source detection algorithm in Section 3. In Section 4, we evaluate the finite sample performance of our proposed method via simulation studies. Further, the application to predict U.S. presidential elections with transfer learning is conducted in Section 5. Section 6 establishes the estimation convergence rates of the transfer learning estimators for the SAR model and derive the detection consistency of the transferable source detection algorithm. We conclude the paper in Section 7. Additional simulation results, theoretical analysis, and all proofs are provided in the supplementary materials.

Notations. Let $[n] \equiv \{1, \ldots, n\}$. For an index set $\mathcal{A} \subseteq [K]$ and a sequence of positive integers $\{n_k, k = 1, \ldots, K\}$, $n_{\mathcal{A}} \equiv \sum_{k \in \mathcal{A}} n_k$. For a vector $\mathbf{x} \in \mathbb{R}^d$ and S being a subset of set $[d]$, $\mathbf{x}_S$ is the sub-vector of $\mathbf{x}$ with index S. The notation $a \lesssim b$ means there exists a positive constant C s.t. $a \leq Cb$. The notation $a \vee b$ means $\max(a, b)$, and $a \wedge b$ means $\min(a, b)$. The notation $a_n \asymp b_n$ means that a_n/b_n converges to a positive constant. For any random sequences a_n and b_n, $b_n = O_{\mathbb{P}}(a_n)$ means $\forall \epsilon > 0, \exists M > 0$ s.t. $\limsup_n \mathbb{P}(|b_n| \geq M|a_n|) \leq \epsilon$, and

$a_n \ll b_n$ means $|a_n| = o_{\mathbb{P}}(|b_n|)$, i.e. $\lim_{n \to \infty} \mathbb{P}(|\frac{a_n}{b_n}| \geq \varepsilon) = 0$ for any $\varepsilon > 0$. For a vector $\mathbf{x} = (x_1, \ldots, x_d)^{\mathsf{T}} \in \mathbb{R}^d$, we define $\|\mathbf{x}\|_1 = \sum_{j=1}^{d} |x_j|$, $\|\mathbf{x}\|_2 = (\sum_{j=1}^{d} x_j^2)^{1/2}$, and $\|\mathbf{x}\|_\infty = \max_{1 \leq j \leq d} |x_j|$. For two column vectors $\mathbf{x}$ and $\mathbf{y} \in \mathbb{R}^d$, their inner product is $\langle \mathbf{x}, \mathbf{y} \rangle = \mathbf{x}^{\mathsf{T}} \mathbf{y}$. For an $n \times n$ matrix A, we define $\|A\|_F \equiv (\sum_{i=1}^{m} \sum_{j=1}^{n} |a_{ij}|^2)^{1/2}$, $\|A\|_\infty \equiv \max_i \sum_{j=1}^{n} |a_{ij}|$, its spectral norm $\|A\|_2 \equiv \max_{x \in \mathbb{R}^n \setminus \{0\}} \frac{\|Ax\|_2}{\|x\|_2} = \sqrt{\lambda_{\max}(A'A)}$, where $\lambda_{\max}(A)$ is the maximum eigenvalue of A and $\lambda_{\min}(A)$ is the minimum eigenvalue of A. For an $n \times m$ matrix A, $A_{(i,j)}$ represents the element in its i-th row and j-th column. $A_{(\cdot,j)}$ refers to the j-th column of A, and $A_{(i,\cdot)}$ represents the i-th row of matrix A.

2 Problem and Model Settings

In this work, we focus on predicting the U.S. presidential election results of each county in swing states by incorporating the spatial relationship among counties. We try to predict the election results in 2020 and 2024 elections using the polls from the 2016 and 2020 election U.S. presidential election and some other demographic data and geographic data, respectively. It is worth noting that swing states have undergone historical shifts over time. The process of identifying swing states in previous elections typically involves an assessment of the closeness of the vote margins in each state. This analysis incorporates historical election outcomes, opinion polls, political trends, recent developments since the previous election, and the specific attributes, strengths, or vulnerabilities of the candidates in contention. In Section 2.1, we describe the motivation problem and data. Here, we reiterate the challenges we face, namely the utilization of spatial information and data scarcity. To this end, we propose a novel transfer learning framework based on the SAR model aimed at addressing above mentioned two challenges.

2.1 Problem and Data

Problem: We aim to handle the challenges of utilizing spatial information and analyzing spatial factors in predicting the U.S. presidential election. From Figure 1, it is evident that the county-level support rates in the U.S. presidential election display a spatial relationship. Spatial relationships among the data are also prevalent, making it essential to incorporate spatial information into the analysis. In U.S. presidential elections, the distribution of votes exhibits significant spatial dependency, a phenomenon particularly obvious over counties. Specifically, the voting patterns of a county tend to align closely with those of its neighboring counties. This similarity can often be attributed to the shared socio-economic characteristics that arise from geographical proximity, such as industrial structure, income levels, and educational attainment (Fotheringham et al., 2021; Kim et al., 2003). Additionally, whether a county is urban or rural plays a substantial role in this spatial dependency. Urban counties generally show stronger support for the Democratic Party, whereas suburban and rural counties tend to favor the Republican Party. Thus, in analyzing voting distributions, the urban or rural status of a county becomes a critical factor, reflecting not only the geographical distribution of political preferences but also highlighting the political and social divides between urban and rural areas. Recognizing this spatial dependency helps in more accurately predicting election outcomes and in forming strategies for political parties. Thus the first challenge lies in how to incorporate spatial information into transfer learning techniques. Though the method proposed by Tian and Feng (2023) provides a valuable framework to transfer learning and has been applied to the U.S. presidential election, their method is for independent data and does not account for spatial information during transfer learning. Furthermore, the second challenge is the issue of data scarcity. It is evident that the average sample size per state (the number of counties) is only around 60. Relying only on data from swing states for spatial analysis could harm the accuracy of the estimates.
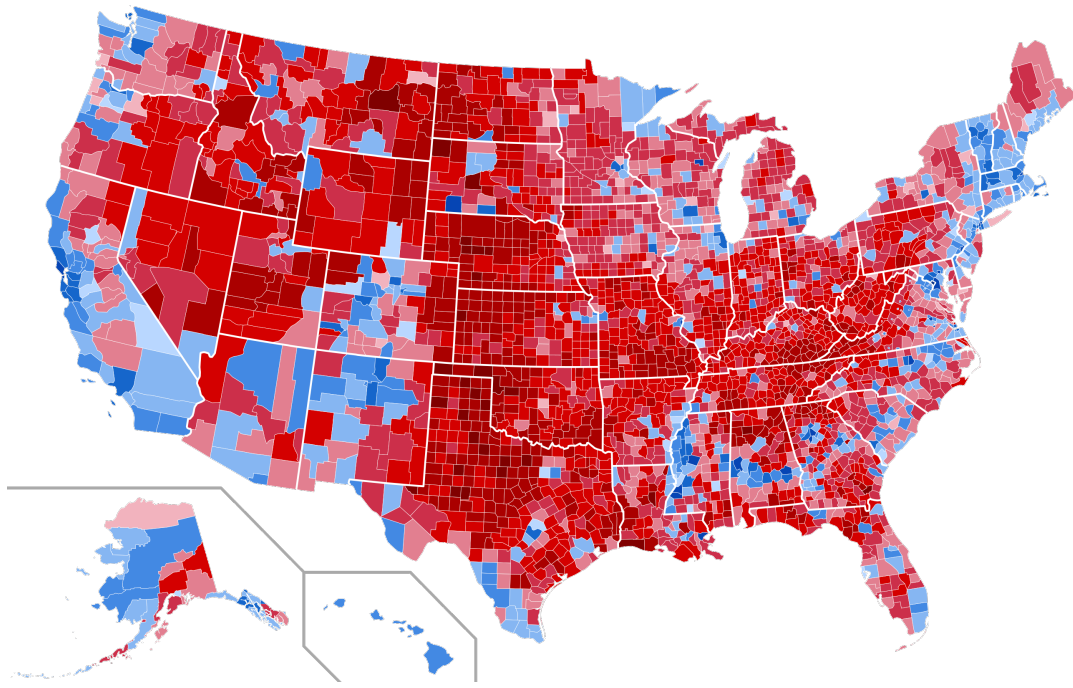
Figure 1: Results by county of the 2020 United States presidential election (Magog the Ogre, 2020). The red areas represent support for Trump, while the blue areas indicate support for Biden. The intensity of the color corresponds to the degree of support.

Data sources and processing: The digital boundary definitions of the United States congressional district are available at `https://cdmaps.polisci.ucla.edu/`, and the cartographic boundary shape files of counties in the USA are available at the United States Census Bureau (`https://www2.census.gov/geo/tiger/`). The spatial weight matrix is constructed using above two geographic datasets. Here we apply the "queen" contiguity-based spatial weights and row-normalized. The "queen" criterion defines neighbors as spatial units sharing a common edge or a common vertex. The response is the difference of support at the county level for presidential candidates from both parties in 2016 and 2020, available at `https://github.com/tonmcg/US_County_Level_Election_Results_08-20`. The county-level demographic information forms the predictors, collected at `https://data.census.gov/`. Among all states and the federal district, we exclude Alaska, Hawaii, and Washington, D.C.. In these 48 states, there are 3107 counties and we have 142 county-level predictors.

2.2 Model Settings

In order to deal with the two aforementioned challenges in U.S. presidential election prediction problems, we present a transfer learning framework within the spatial autoregressive (SAR) model. For a pre-specified swing state as the target data, we consider the following SAR model,

$$Y^{(0)} = \sum_{l=1}^{p} \lambda_{l0} W_l^{(0)} Y^{(0)} + \sum_{j=1}^{q} X_j^{(0)} \beta_{j0} + V^{(0)}, \tag{1}$$

where the difference of support $Y^{(0)}$ is an $n_0 \times 1$ vector of spatially correlated dependent variables, $W_l^{(0)}$ is an $n_0 \times n_0$ known non-stochastic spatial weight matrix for each $l \in [p]$, the county-level demographic information $X_j^{(0)}$ is an $n_0 \times 1$ vector of exogenous regressors independent of the error term $V^{(0)}$ for each $j \in [q]$, $V^{(0)}$ is an $n_0 \times 1$ vector of independently and identically distributed (i.i.d.) random variables with mean 0 and variance $\sigma^2 > 0$. Let $\lambda_0 = (\lambda_{10}, \ldots, \lambda_{p0})^\mathsf{T}$, $\beta_0 = (\beta_{10}, \ldots, \beta_{q0})^\mathsf{T}$ and $\theta_0 \equiv (\lambda_0^\mathsf{T}, \beta_0^\mathsf{T})^\mathsf{T}$.

Similar to general transfer learning settings as in Bastani (2021), Li et al. (2021), Tian and Feng (2023), in addition to the target study (1), additional samples are obtained from K auxiliary studies (also termed as *source datasets*) from other states, where K is assumed to be fixed. For the k-th source dataset, we also consider the SAR model,

$$Y^{(k)} = \sum_{l=1}^{p} \lambda_{l0}^{(k)} W_l^{(k)} Y^{(k)} + \sum_{j=1}^{q} X_j^{(k)} \beta_{j0}^{(k)} + V^{(k)}, \ k \in [K], \tag{2}$$

where $Z^{(k)} \equiv (Y^{(k)}, X_1^{(k)}, \ldots, X_q^{(k)})$ is the k-th source dataset of sample size n_k, $W_l^{(k)}$ is an $n_k \times n_k$ non-stochastic spatial weight matrix for each $l \in [p]$, and $V^{(k)}$ is an $n_k \times 1$ vector of i.i.d. random variables with mean zero and variance σ_k^2, independent of the covariates $X_j^{(k)}, j \in [q]$. Let $\lambda_0^{(k)} = (\lambda_{10}^{(k)}, \ldots, \lambda_{p0}^{(k)})^\mathsf{T}$, $\beta_0^{(k)} = (\beta_{10}^{(k)}, \ldots, \beta_{q0}^{(k)})^\mathsf{T}$ and $\omega_0^{(k)} \equiv (\lambda_0^{(k)\mathsf{T}}, \beta_0^{(k)\mathsf{T}})^\mathsf{T}$ for the k-th source dataset. Let $\mathbf{X}^{(k)} \equiv (X_1^{(k)}, \ldots, X_q^{(k)})$, $\mathbf{W}^{(k)} \equiv (W_1^{(k)}, \ldots, W_p^{(k)})$, and $\mathfrak{D}^{(k)} \equiv (Y^{(k)}, \mathbf{X}^{(k)}, \mathbf{W}^{(k)})$, $k = 0, \ldots, K$. In transfer learning, a similar auxiliary model to the target model is called an *informative* model, and the "similarity" is characterized by the difference between $\omega_0^{(k)}$ and θ_0, i.e. $\delta^{(k)} \equiv \theta_0 - \omega_0^{(k)}$.

Given a tolerance level $h > 0$, the index set of the informative auxiliary samples is defined as

$$\mathcal{A} \equiv \mathcal{A}_h = \{0 \le k \le K : \|\delta^{(k)}\|_1 \le h\}, \tag{3}$$

where $\|\delta^{(k)}\|_1$ is called the *transferring level* of the k-th source dataset. In this context, the value of h is used to balance the bias and the variance introduced by transfer learning. When h is large, more labeled datasets are used, which reduces the prediction variance but increases the bias due to source datasets, and vice versa. We will discuss the value of h in the conditions for theoretical results in Section 6.

3   Statistical Methodology

3.1   Estimation with known informative source data

In this section, we propose a two-step transfer learning procedure under the SAR model when the index set $\mathcal{A}_h$ of the informative auxiliary samples is known, denoted as $\mathcal{A}$-*TranSAR*. In the first transferring step, we consolidate information from various sources by pooling all available auxiliary data, yielding a preliminary estimator which is typically biased, since $\omega_0^{(k)} \neq \theta_0$ in general, although they are close. In the second debiasing step, we correct the estimation bias by incorporating the target data via regularization. The details of the two-stage estimation procedure are present in the following.

The transferring stage   The first-step estimator, which is also called *pre-training* model in the transfer learning literature, with tuning parameter λ_ω is defined as

$$\widehat{\omega} = \arg\min_{\omega \in \mathbb{R}^{p+q}} \left\{ \frac{1}{2n_{\mathcal{A}}} \sum_{k \in \mathcal{A}} \ell_1 \left(\mathfrak{D}^{(k)} \mid \omega \right) + \lambda_\omega \|\omega\|_1 \right\}, \tag{4}$$

where $\ell_1(\cdot \mid \omega)$ is a generic loss function with parameter ω, and $n_{\mathcal{A}} \equiv \sum_{k \in \mathcal{A}} n_k$ is the total sample size of all informative source data. For the SAR model, the estimator could be the two-stage

least squares (2SLS) estimator (Kelejian and Prucha, 1998; Lee, 2003), generalized method of moments estimator (GMM) (Kelejian and Prucha, 1999; Lee, 2007; Liu and Lee, 2010), quasi-maximum likelihood estimator (Lee, 2004, QMLE) and so on. The main requirement for the first step estimator is a suitable convergence rate discussed in detail in Section 6. Here the tuning parameter λ_ω could be zero in low dimensional cases. When the dimension of parameters is greater than the sample size in high dimensional cases, the penalized SAR estimation with nonzero λ_ω could produce a sparse estimator(Higgins and Martellosio, 2023). See also Zhang and Yu (2018) for spatial weight matrices selection with model averaging, and Tibshirani (1996); Fan and Li (2001); Zhang (2010); Wang et al. (2011); Su et al. (2017) for more detail in regularization method.

Remark 1. The index set $\mathcal{A}$ may or may not contain the index 0. This depends on the actual application scenarios. In some cases the source data are available, and in the other cases, it may be difficult to obtain due to data privacy protection and security considerations. In the latter case, the owner of the source data can provide the estimation results obtained by the first stage learner without the target data instead of the original source data, and the target task will use this result for the next debiasing stage.

The debiasing stage In the second step, the bias term estimator $\widehat{\delta}$ with tuning parameter λ_δ using the target data is defined as

$$\underset{\delta \in \mathbb{R}^{p+q}}{\arg\min} \frac{1}{2n_0} \ell_2 \left(\mathfrak{D}^{(0)} \mid \widehat{\omega} + \delta \right) + \lambda_\delta \|\delta\|_1. \tag{5}$$

Then, the bias-corrected $\mathcal{A}$-*TranSAR* estimator is defined as

$$\widehat{\theta}_{\mathcal{A}\text{-}TranSAR} = \widehat{\omega} + \widehat{\delta}. \tag{6}$$

The two-stage transfer learning procedure under the SAR model is summarized in Algorithm 1.

Algorithm 1: $\mathcal{A}$*-TranSAR*

Input: target dataset: $\mathfrak{D}^{(0)}$; sources datasets: $(\mathfrak{D}^{(k)}, k \in \mathcal{A})$; transferring set: $\mathcal{A}$; and tuning parameters: λ_ω and λ_δ

Output: $\hat{\theta}_{\mathcal{A}\text{-}TranSAR}$

1 The transferring stage:

$$\widehat{\omega} = \underset{\omega \in \mathbb{R}^{p+q}}{\arg\min} \left\{ \frac{1}{2n_\mathcal{A}} \sum_{k \in \mathcal{A}} \ell_1\left(\mathfrak{D}^{(k)} \mid \omega\right) + \lambda_\omega \|\omega\|_1 \right\}$$

2 The debiasing stage:

$$\widehat{\delta} = \underset{\delta \in \mathbb{R}^{p+q}}{\arg\min} \frac{1}{2n_0} \ell_2\left(\mathfrak{D}^{(0)} \mid \widehat{\omega} + \delta\right) + \lambda_\delta \|\delta\|_1.$$

3 Output: $\widehat{\theta}_{\mathcal{A}\text{-}TranSAR} = \widehat{\omega} + \widehat{\delta}$

Remark 2. The loss functions ℓ_1 and ℓ_2 in the two stages are allowed to be different. In fact, we make no specific requirements on the form of ℓ_1 as long as the resulting estimator in the transferring stage satisfies the certain convergence rates discussed in Section 3.

In particular, we consider a classical 2SLS procedure in the second stage as an example, which has been widely used for the SAR model to deal with the endogeneity. Given an $n_0 \times d$ $(d \geq p+q)$ instrumental variables matrix $Q^{(0)}$ containing $\mathbf{X}^{(0)}$, the first-stage estimator in the 2SLS procedure is

$$\widehat{\pi}_j = \underset{\pi_j \in \mathbb{R}^d}{\arg\min} \left\{ \frac{1}{2n_0} \|\mathbb{X}_j^{(0)} - Q^{(0)}\pi_j\|_2^2 \right\}, \tag{7}$$

for each $j \in [p+q]$, where $\mathbb{X}^{(0)} = (W_1^{(0)}Y^{(0)}, \ldots, W_p^{(0)}Y^{(0)}, \mathbf{X}^{(0)}) \in \mathbb{R}^{n_0 \times (p+q)}$, $\mathbb{X}_j^{(0)}$ is the j-th column of $\mathbb{X}^{(0)}$ and π_j's are coefficients of instrumental variables. Denote the fitted values of $\mathbb{X}_j^{(0)}$'s by $\widehat{\mathbb{X}}_j^{(0)} \equiv Q^{(0)}\widehat{\pi}_j = P_{Q^{(0)}}\mathbb{X}_j^{(0)}$, and $\widehat{\mathbb{X}}^{(0)} = (\widehat{\mathbb{X}}_1^{(0)}, \ldots, \widehat{\mathbb{X}}_{p+q}^{(0)})$, where the projection matrix is $P_{Q^{(0)}} \equiv Q^{(0)}(Q^{(0)\mathsf{T}}Q^{(0)})^{-1}Q^{(0)\mathsf{T}}$. In the SAR model, instrumental variables could be

$$Q^{(0)} = (\mathbf{X}^{(0)}, W_1^{(0)}\mathbf{X}^{(0)}, \ldots, W_p^{(0)}\mathbf{X}^{(0)})$$

with $d = q(1+p)$ columns. We note that if the first column of $\mathbf{X}^{(0)}$ is the intercept term 1, we need to drop it in $W_j^{(0)}\mathbf{X}^{(0)} (j \in [p])$ to avoid multicollinearity. See Kelejian and Prucha (1998)

and Lee (2003) for several alternative choices of instruments. The corresponding loss function for the second stage estimation is

$$\ell_2\left(\mathfrak{D}^{(0)} \mid \theta\right) = \|Y^{(0)} - \widehat{\mathbb{X}}^{(0)}\theta\|_2^2. \tag{8}$$

Then, the bias-corrected $\mathcal{A}$-*TranSAR* estimator can be equivalently obtained by

$$\widehat{\theta}_{\mathcal{A}\text{-}TranSAR} = \underset{\theta \in \mathbb{R}^{p+q}}{\arg\min} \frac{1}{2n_0} \ell_2\left(\mathfrak{D}^{(0)} \mid \theta\right) + \lambda_\delta \|\theta - \widehat{\omega}\|_1. \tag{9}$$

Remark 3. For high dimensional settings in the reduced form, the number of instruments is larger than the sample size. We could consider using a penalized 2SLS procedure as

$$\widehat{\pi}_j = \underset{\pi_j \in \mathbb{R}^d}{\arg\min} \left\{ \frac{1}{2n_0} \|\mathbb{X}_j^{(0)} - Q^{(0)}\pi_j\|_2^2 + p_{\lambda_{\pi_j}}(\pi_j) \right\}, \tag{10}$$

for certain penalty function $p_{\lambda_{\pi_j}}(\cdot)$. In the literature, Belloni et al. (2012) proposed the implementation of Lasso and post-Lasso methods to form the first-stage predictions and estimate optimal instruments in a linear instrumental variables model. Fan and Liao (2014) developed a novel penalized GMM to cope with the endogeneity of a high dimensional model. Cheng and Liao (2015) studied the problem of choosing valid and relevant moments for GMM estimation and developed asymptotic results for high-dimensional GMM shrinkage estimators that allow for non-smooth sample moments and weakly dependent observations. Zhu (2018) and Gold et al. (2020) introduced a two-stage Lasso procedure and established some finite-sample convergence rates under different assumptions.

3.2 A transferable source detection algorithm

The $\mathcal{A}$-*TranSAR* estimator requires the true informative index set $\mathcal{A}$ to be known correctly. However, in most empirical applications, the true informative set $\mathcal{A}$ is unknown. Transferring adversarial auxiliary samples may not improve the performance of the target model and could even cause worse results. The effect of adversarial auxiliary samples is also called *negative transfer*, meaning

that certain inferior results are caused by uninformative source data (Torrey and Shavlik, 2010; Tian and Feng, 2023).

An intuitive approach might involve seeking a metric of similarity between each source and the target data. We compute the initial loss based on the target dataset. Subsequently, we combine the target dataset with each source dataset individually to estimate and compute the corresponding losses. If a source dataset is similar to the target dataset, we anticipate two loss values to be comparably close. Hence, we select a critical value to identify which source datasets are informative. For spatial datasets characterized by a network structure, data splitting used in Tian and Feng (2023) can not be directly applied since it could disrupt this network integrity. As a result, we introduce the spatial residual bootstrap approach as an alternative. This idea is illustrated in details as follows.

First, we compute an initial estimator $\widehat{\theta}_{ini} = (\widehat{\lambda}_{ini}^{\mathsf{T}}, \widehat{\beta}_{ini}^{\mathsf{T}})^{\mathsf{T}}$ using the target samples by certain estimation methods, such as 2SLS, QMLE or GMM, etc. Then, we obtain the residuals $\hat{e} = Y^{(0)} - \mathbb{X}^{(0)}\hat{\theta}_{ini}$, where $\mathbb{X}^{(0)} = (W_1^{(0)}Y^{(0)}, \ldots, W_p^{(0)}Y^{(0)}, \mathbf{X}^{(0)})$. Similar to residual bootstrap, we generate three independent copies, $\widehat{e}^{(1)}$, $\widehat{e}^{(2)}$ and $\widehat{e}^{(3)}$ of sample size n_0 from the empirical distribution of $\widehat{e}$. Then, we generate three-fold bootstrap samples $Y^{(0,r)}$ and $\mathbf{X}^{(0,r)}$ by

$$Y^{(0,r)} = \mathbb{X}^{(0)}\widehat{\theta}_{ini} + \widehat{e}^{(r)}, \quad \mathbf{X}^{(0,r)} = \mathbf{X}^{(0)}, \tag{11}$$

for $r = 1, 2, 3$. Let $Z^{(0,r)} = (Y^{(0,r)}, \mathbf{X}^{(0,r)})$ for $r = 1, 2, 3$. Let $Z^{(0,-r)}$ be the concatenated bootstrap samples without the r-th sample, for example, $Z^{(0,-1)} = (Z^{(0,2)\mathsf{T}}, Z^{(0,3)\mathsf{T}})^{\mathsf{T}}$. Define $\mathbf{X}^{(0,-r)}, \mathbb{X}^{(0,r)}$ and $\mathbb{X}^{(0,-r)}$ similarly.

Second, for each $r = 1, 2, 3$, we fit the model in (1) on the connected bootstrap samples $Z^{(0,-r)}$ and use the resulting estimator $\widehat{\theta}^{(0,r)}$ to compute the loss value on the remaining bootstrap sample $Z^{(0,r)}$, that is

$$\mathcal{L}^{[r]}(\widehat{\theta}^{(0,r)}) \equiv \frac{1}{2n_0}\|Y^{(0,r)} - \mathbb{X}^{(0,r)}\widehat{\theta}^{(0,r)}\|_2^2. \tag{12}$$

14

Then, we compute the average of three loss values, $\mathcal{L}^{(0)} = \sum_{r=1}^{3} \mathcal{L}^{[r]}(\widehat{\theta}^{(0,r)})/3$, which serves as the baseline loss value for the target dataset. We can also compute the standard deviation of three loss values, denoted by

$$\hat{\sigma} = \sqrt{\frac{1}{2} \sum_{r=1}^{3} \left(\mathcal{L}^{[r]}(\widehat{\theta}^{(0,r)}) - \mathcal{L}^{(0)} \right)^2}, \tag{13}$$

which measures the dispersion of bootstrapped loss values $\mathcal{L}^{[r]}(\widehat{\theta}^{(0,r)})$ relative to their average $\mathcal{L}^{(0)}$. Next, for each $r = 1, 2, 3$, we combine $Z^{(0,-r)}$ with each k-th source dataset, fit the model in (1) on the newly combined data and compute the loss denoted by $\mathcal{L}^{(k,r)}$ on $Z^{(0,r)}$. Similarly, the average loss for the k-th source dataset over three-fold bootstrap samples is $\mathcal{L}^{(k)}$. Consequently, the difference between $\mathcal{L}^{(k)}$ and $\mathcal{L}^{(0)}$ provides a metric of the similarity between the k-th source dataset and the target data. Source datasets whose corresponding loss differences below certain threshold are recognized as transferable informative data. Following the idea of Tian and Feng (2023), we choose $\hat{\sigma} \vee 0.01$ as the detection threshold. Then, the estimated transferable source index set $\widehat{\mathcal{A}}$ is defined as

$$\widehat{\mathcal{A}} = \left\{ k = 1, \ldots, K \mid \mathcal{L}^{(k)} - \mathcal{L}^{(0)} \leq (\hat{\sigma} \vee 0.01) \right\}. \tag{14}$$

Once the transferable set $\mathcal{A}$ is estimated, we can apply the $\mathcal{A}$-*TranSAR* in Algorithm 1 to obtain the transfer learning estimator for the SAR model, denoted by $\widehat{\theta}_{\widehat{\mathcal{A}}\text{-}TranSAR}$, which is termed as the *TranSAR* estimator. The procedure described above is summarized in Algorithm 2.

4   Simulation

In this section, we design several simulation experiments to investigate the performance of the proposed method (denoted as *TranSAR*). We compare the finite sample performance of our estimator with the classical 2SLS estimation (which is fitted only using the target dataset, denoted as *SAR*), the $\mathcal{A}$-*TranSAR* estimator (which is fitted based on the true informative index set $\mathcal{A}$, denoted as *Oracle TranSAR*), pooled-estimator (which is fitted using all the source datasets as

---
Algorithm 2: *TranSAR*

Input: target: $\mathfrak{D}^{(0)}$; all sources: $(\mathfrak{D}^{(k)}, k \in [K])$; tuning parameter: $\lambda_{\theta}^{(k,r)}, k \in [K] \cup \{0\}, r \in [3]$; an initial estimator, $\widehat{\theta}_{ini}$.

Output: $\widehat{\theta}_{TranSAR}$ and $\widehat{\mathcal{A}}$.

1 Residuals: $\hat{e} = Y^{(0)} - \mathbb{X}^{(0)}\hat{\theta}_{ini}$;

2 for r *from* 1 *to* 3 **do**

3 $\quad$ Generate an independent copy $\hat{e}^{(r)}$ from $\hat{e}$ and $Y^{(0,r)}$, $\mathbf{X}^{(0,r)}$, $Z^{(0,-r)}$, $\mathbf{X}^{(0,-r)}$, $\mathbb{X}^{(0,r)}$ and $\mathbb{X}^{(0,-r)}$;

4 $\quad$ $\widehat{\theta}^{(0,r)} \leftarrow \underset{\theta \in \mathbb{R}^{p+q}}{\arg\min} \frac{1}{2n_0} \ell_2\left(Z^{(0,-r)} \mid \theta\right) + \lambda_{\theta}^{(0,r)}\|\theta\|_1$;

5 $\quad$ **for** k *from* 1 *to* K **do**

6 $\quad\quad$ $\widehat{\theta}^{(k,r)} \leftarrow \underset{\theta \in \mathbb{R}^{p+q}}{\arg\min} \left\{ \frac{1}{2(n_k+2n_0)} \left\{ \ell_2(\mathfrak{D}^{(k)} \cup Z^{(0,-r)} \mid \theta) \right\} + \lambda_{\theta}^{(k,r)}\|\theta\|_1 \right\}$;

7 $\quad$ **end**

8 end

9 Calculate the average losses: $\mathcal{L}^{(k)} = \frac{1}{3}\sum_{r=1}^{3}\mathcal{L}^{[r]}(\hat{\theta}^{(k,r)}), k = 0, 1, \ldots, K$;

10 Calculate the standard deviation: $\hat{\sigma} \leftarrow \sqrt{\frac{1}{2}\sum_{r=1}^{3}\left(\mathcal{L}^{[r]}(\hat{\theta}^{(0,r)}) - \mathcal{L}^{(0)}\right)^2}$;

11 The estimated transferable source index set:

$\quad \hat{\mathcal{A}} \leftarrow \left\{ k = 1, \ldots, K \mid \mathcal{L}^{(k)} - \mathcal{L}^{(0)} \leq (\hat{\sigma} \vee 0.01) \right\}$;

12 $\widehat{\theta}_{TranSAR}$ is obtained by Algorithm 1 via letting $\mathcal{A} = \hat{\mathcal{A}}$;

---

the transferable sets, denoted as [K]-*TranSAR*), and the generalized linear model transfer learning algorithm (denoted as *glmtrans*) proposed by Tian and Feng (2023). The *glmtrans* ignores the spatial information and can be considered as a baseline estimator to show that it is necessarily important to consider the spatial correlations if they exist.

We generate the data according to Models (1) and (2). In these models, $n_0 = 256, n_1 = n_2 = \cdots = n_K = 100, p = 1, q = 200, K = 20$. The covariates $\mathbf{x}_i^{(k)}$ are generated by multivariate normal distribution with covariance matrix $\Sigma \in \mathbb{R}^{q \times q}$, whose the (j, j')-th entry is denoted as $\Sigma_{j,j'}$ for all $0 \leq k \leq K$. We consider three designs for Σ: (1) $\Sigma_{j,j'} = 1$ for $j = j'$ and $\Sigma_{j,j'} = 0$ otherwise, (2) $\Sigma_{j,j'} = 0.5^{|j-j'|}$, (3) $\Sigma_{j,j'} = 0.9^{|j-j'|}$. We consider two different distributions for the i.i.d. error terms: (1) the standard normal distribution $N(0,1)$, and (2) the t_2 distribution. The spatial units are assumed to be located on a square grid, and we set up several candidate spatial weight matrices as follows: (1) the first W_1 is the spatial weight matrix where spatial units interact with their

neighbors on the left and right sides; (2) the second W_2 is the spatial weight matrix where spatial units interact with their neighbor above and below; (3) the rest of the spatial weight matrices are assumed to be matrices where spatial units interact with their second-nearest, third-nearest, and so on, denoted as $W_3, \ldots, W_N$, where $N < \sqrt{n_0}$. In each dataset, we randomly draw spatial weight matrices from these candidate matrices. The weight matrices $\{W_{k,l}\}_{k \in \{0\} \cup [K], l \in [p]}$ are drawn randomly from $\{W_1, \ldots, W_N\}$ without replacement. In Models (1) and (2), we consider coefficients settings as follows. In the target Model (1), $\lambda_0 = 0.4$ and $\beta_0 = (\mathbf{1}_3^\intercal, \mathbf{0}_{q-3}^\intercal)^\intercal \in \mathbb{R}^q$. In Model (2),

$$\lambda_0^{(k)} = \lambda_0 \mathbb{1}\{k \in \mathcal{A}\} - \lambda_0 \mathbb{1}\{k \in \mathcal{A}^c\},$$

$$\beta_{j0}^{(k)} = \beta_{j0} - 0.05\mathbb{1}\{j \in \mathcal{H}_k, k \in \mathcal{A}\} - 2\mathbb{1}\{j \in \mathcal{H}_k, k \in \mathcal{A}^c\}, j = 1, \ldots, q,$$

where $\mathcal{H}_k$ is a random subset of $[q]$ with $|\mathcal{H}_k| = H$ if $k \in \mathcal{A}$ (i.e., H is the number of different coefficients in the informative set), or $|\mathcal{H}_k| = \frac{q}{2}$ if $k \notin \mathcal{A}$. So, on the informative datasets, the differences of different $\beta_{j0}^{(k)}$'s are 0.05; on uninformative datasets, the ones of different $\beta_{j0}^{(k)}$'s are 2.

We compute the root mean squared errors (RMSE),

$$\text{RMSE} = \sqrt{\frac{1}{R} \sum_{r=1}^{R} \|\theta_0 - \widehat{\theta}^{[r]}\|^2}, \tag{15}$$

where $\widehat{\theta}^{[r]}$ is the estimator of the r-th replication, based on the 2SLS loss with $q = 200$ and display them under different settings in Figure 2. In order to demonstrate the advantages of transfer learning, we let the size of informative auxiliary datasets $|\mathcal{A}|$ increase from 0 to 20 to show the decreasing trend in RMSE. As the number of informative sets increases, compared to the classical 2SLS estimation and the *glmtrans* method, we can see that $\widehat{\mathcal{A}}$-*TranSAR* and $\mathcal{A}$-*TranSAR* can significantly reduce the RMSE, resulting in more precise estimation. Additionally, we can see that the $\widehat{\mathcal{A}}$-*TranSAR* performs almost the same as the oracle transfer learning method $\mathcal{A}$-*TranSAR*. That means, our proposed detection method is able to select informative sets with a high probability. Moreover, from Figure 2, when the number of informative sets is small, the negative

transfer effect of the pooled method, $[K]$-$TranSAR$ becomes apparent. Hence, it is necessary to select informative sets accurately. The same conclusion applies to all three types of design matrices and the three different settings for H. Detailed and comprehensive simulation results are compiled in Table 1 for covariates designs type 1.
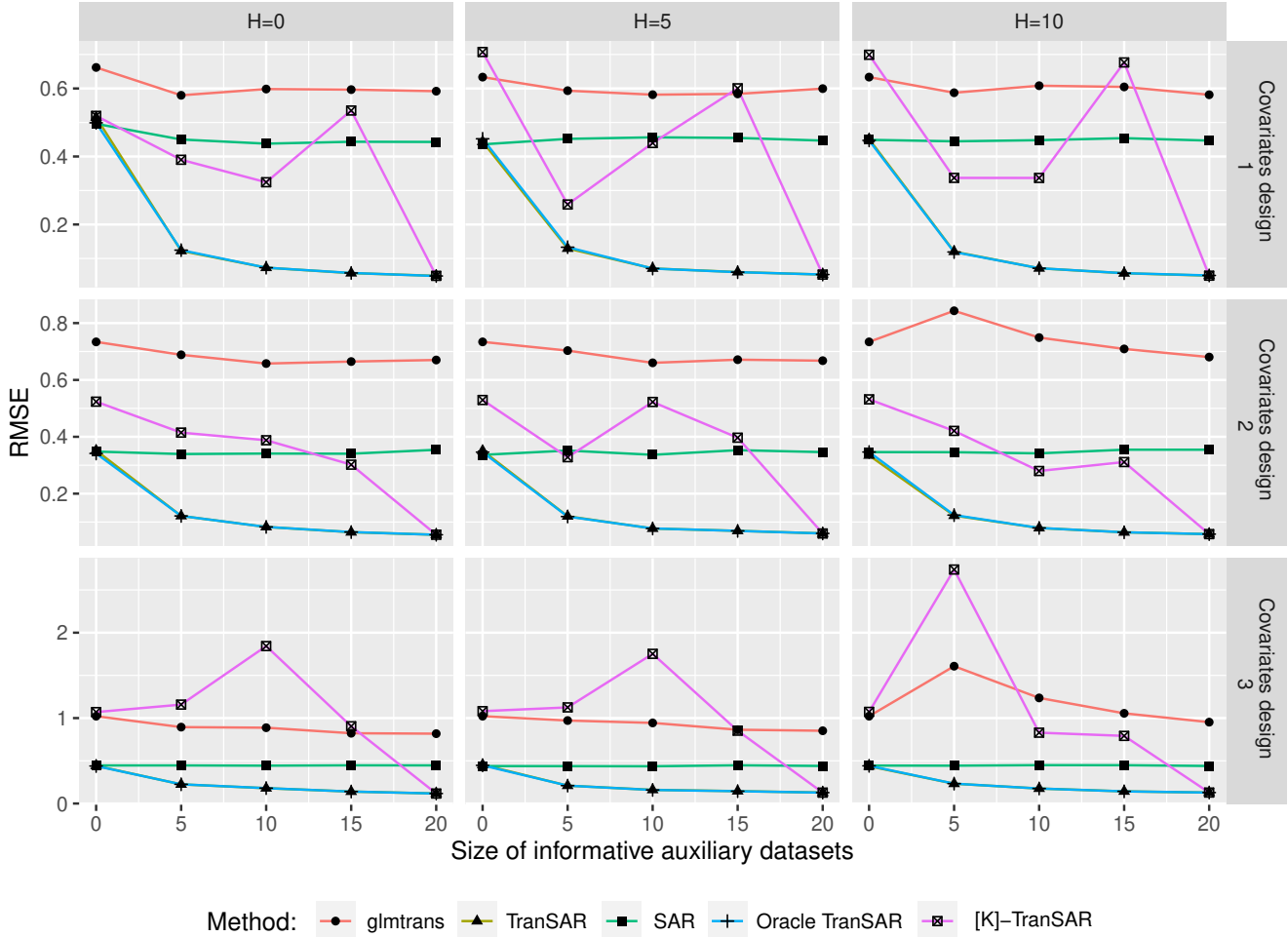

Figure 2: RMSE of Three Types of Covariates Designs with Normal Error Distribution, and $H = 0, 5, 10$.

5   An Application to U.S. Presidential Election Prediction

In this section, we apply the proposed method in Algorithm 2 to empirical data from the U.S. presidential election. As shown in Section 2.1, the response variable $Y^{(k)}$ is the difference of

$|\mathcal{A}_h|$	Method	H=0		H=5		H=10	
		RMSE of $\widehat{\lambda}$	Total RMSE	RMSE of $\widehat{\lambda}$	Total RMSE	RMSE of $\widehat{\lambda}$	Total RMSE
Covariates design 1							
$|\mathcal{A}_h| = 0$	SAR	0.01931	0.49616	0.01593	0.44895	0.01507	0.43567
	$[K]$-TranSAR	0.03309	0.51944	0.03755	0.69910	0.03892	0.70725
	glmtrans	NA	0.66184	NA	0.63342	NA	0.63342
	TranSAR	0.02088	0.51506	0.01574	0.45135	0.01574	0.44359
	Oracle TranSAR	0.01938	0.49908	0.01556	0.44738	0.01638	0.45203
$|\mathcal{A}_h| = 10$	SAR	0.01536	0.43773	0.01568	0.44799	0.01633	0.45635
	$[K]$-TranSAR	0.07954	0.32422	0.07143	0.33693	0.06139	0.43960
	glmtrans	NA	0.59838	NA	0.60811	NA	0.58176
	TranSAR	0.00868	0.07301	0.00842	0.07117	0.00842	0.07073
	Oracle TranSAR	0.00873	0.07296	0.00835	0.07138	0.00844	0.07052
$|\mathcal{A}_h| = 20$	SAR	0.01552	0.44279	0.01598	0.44674	0.01568	0.44669
	$[K]$-TranSAR	0.00643	0.04898	0.00692	0.04951	0.00614	0.05267
	glmtrans	NA	0.59203	NA	0.58152	NA	0.59955
	TranSAR	0.00648	0.04909	0.00693	0.04963	0.00613	0.05275
	Oracle TranSAR	0.00642	0.04853	0.00698	0.05011	0.00614	0.05288
Covariates design 2							
$|\mathcal{A}_h| = 0$	SAR	0.01284	0.34807	0.01256	0.34623	0.01203	0.33645
	$[K]$-TranSAR	0.03664	0.52357	0.03667	0.53178	0.03734	0.52947
	glmtrans	NA	0.73390	NA	0.73390	NA	0.73390
	TranSAR	0.01305	0.35195	0.01173	0.33473	0.01309	0.35113
	Oracle TranSAR	0.01188	0.34144	0.01279	0.34645	0.01280	0.34603
$|\mathcal{A}_h| = 10$	SAR	0.01254	0.34102	0.01179	0.34173	0.01204	0.33671
	$[K]$-TranSAR	0.02236	0.38791	0.02557	0.27970	0.03508	0.52258
	glmtrans	NA	0.65766	NA	0.74894	NA	0.66023
	TranSAR	0.00615	0.08292	0.00586	0.07913	0.00561	0.07733
	Oracle TranSAR	0.00605	0.08292	0.00581	0.07938	0.00567	0.07754
$|\mathcal{A}_h| = 20$	SAR	0.01314	0.35434	0.01307	0.35456	0.01282	0.34617
	$[K]$-TranSAR	0.00465	0.05552	0.00479	0.05768	0.00418	0.05992
	glmtrans	NA	0.67016	NA	0.68051	NA	0.66777
	TranSAR	0.00462	0.05539	0.00479	0.05770	0.00420	0.06011
	Oracle TranSAR	0.00462	0.05542	0.00479	0.05763	0.00418	0.06007
Covariates design 3							
$|\mathcal{A}_h| = 0$	SAR	0.01044	0.44594	0.01052	0.44397	0.01006	0.43836
	$[K]$-TranSAR	0.01525	1.07038	0.01479	1.07295	0.01464	1.08117
	glmtrans	NA	1.02237	NA	1.02237	NA	1.02237
	TranSAR	0.01000	0.44203	0.00959	0.43640	0.01076	0.45431
	Oracle TranSAR	0.01002	0.43889	0.01011	0.44119	0.01053	0.44673
$|\mathcal{A}_h| = 10$	SAR	0.01070	0.44301	0.01078	0.44921	0.00960	0.43615
	$[K]$-TranSAR	0.02097	1.84294	0.02474	0.82913	0.02935	1.75217
	glmtrans	NA	0.88731	NA	1.23627	NA	0.94350
	TranSAR	0.00508	0.17931	0.00512	0.17545	0.00493	0.15996
	Oracle TranSAR	0.00508	0.17984	0.00507	0.17543	0.00493	0.15873
$|\mathcal{A}_h| = 20$	SAR	0.01058	0.44641	0.01009	0.43955	0.00990	0.43987
	$[K]$-TranSAR	0.00381	0.11680	0.00413	0.12832	0.00340	0.12749
	glmtrans	NA	0.81752	NA	0.95240	NA	0.85179
	TranSAR	0.00383	0.11714	0.00413	0.12769	0.00340	0.12760
	Oracle TranSAR	0.00382	0.11678	0.00413	0.12836	0.00341	0.12748

Table 1: The RMSE of Various Estimators with Normal Distribution Error Terms. The RMSE of $\widehat{\lambda}$ is the RMSE of the estimated coefficients of the λ_0. The total RMSE is the RMSE of all the estimated coefficients of the covariates. "NA" indicates that "glmtrans" is not applicable for the estimation of λ_0.

support rates in the county level, and covariates $\mathbf{X}^{(k)}$ include demographic and geographica data, such as including total population, total housing units, poverty people population, etc. With the observed spatial weight matrix $\mathbf{W}^{(k)}$, each swing state is regarded as a target with $k = 0$, and all the other states are considered as sources $k \in [47]$. The target model (1) and sources models (2) could formulated as

$$Y^{(k)} = \sum_{l=1}^{p} \lambda_{l0}^{(k)} W_l^{(k)} Y^{(k)} + \sum_{j=1}^{q} X_j^{(k)} \beta_{j0}^{(k)} + V^{(k)}, \; k \in \{0\} \cup [K].$$

We run the proposed estimation method, *TranSAR*, using the polls from the 2016 U.S. presidential election and some other demographic data with geographic information. We also estimate the SAR model with Lasso penalty (due to high dimensional covariates) using only the target datasets (denoted as SAR) to compare the empirical performance. Due to the inherent stochastic nature of the resampling procedure in the algorithm, we conduct multiple replications (20 times) for both methods to obtain a stable result. The average prediction RMSE of the county-level vote results of the county-level 2020 U.S. presidential election is compared at Table 2. For all swing states, the proposed *TranSAR* method performs better than the traditional SAR in terms of RMSE, which demonstrates the necessity of transfer learning in the SAR framework.

	Florida	Georgia	Michigan	Minnesota	North Carolina	Ohio
SAR	0.10723	0.10995	0.10494	0.19211	0.10118	0.10984
tranSAR	0.09417	0.09064	0.08033	0.09646	0.10966	0.08297

Table 2: Average Prediction RMSE of the Predicted County-level Rates of Support in the 2020 Presidential Election.

Moreover, we also consider the practical rules of the U.S. presidential election, which operate on a "winner-takes-all" basis. In this context, the winner party secures all the state's electoral votes. Given the "winner-take-all" framework of the U.S. presidential election, we focus on predicting the

winner party in each state. Leveraging the county-wise population, we compute the final difference of support in the state-level endorsement for presidential contenders belonging to the respective parties. We calculate the rate of support for state-level elections using the following formula,

$$\text{Rate of state-level support} = \sum_i \frac{\text{Rate of county } i \text{ level support} \times \text{Votes of the county } i}{\text{Total votes}}.$$

Then, we compare the prediction rate of state-level support and the true one in 2020 election, showing in Table 3. It demonstrates that the transfer learning under the SAR framework is able to effectively improve the state-level prediction.

	Florida	Georgia	Michigan	Minnesota	North Carolina	Ohio
SAR	-0.01989	-0.08110	-0.07157	-0.04189	-0.01782	-0.05765
tranSAR	0.00546	-0.04186	0.03522	-0.02228	-0.02163	-0.03189

Table 3: Prediction Bias of the Predicted State-level 2020 Election Results.

The calculated ratios of correct predictions out of the 20 election result forecasts are collected in Table 4. As shown in Table 4, the method we proposed exhibits better performance, especially in predicting election outcomes in Michigan and Minnesota. Simultaneously, it is noteworthy that for the election predictions in Georgia, neither of the methods works well. It can be explained by the historical context: from 1972 to 2016, Georgia consistently supported the Republican Party, except for Democratic candidates from the southern region. However, the state has become an increasingly competitive battleground. In 2020, the Democratic candidate, Joe Biden, secured a victory over Donald Trump by a narrow margin of 0.2%. This marks a significant departure from the history, as the Democrats secured the presidential election with a slim advantage. Evidently, Georgia has become an outlier in this regard. It is evident that predicting the ultimate election outcome for a single state is significantly more challenging than forecasting the rate of state-level support. Nevertheless, we have made commendable progress in this regard.

	Florida	Georgia	Michigan	Minnesota	North Carolina	Ohio
SAR	100%	0%	35%	90%	100%	100%
tranSAR	100%	0%	100%	100%	100%	100%

Table 4: The Ratios of Correct Predictions for Election Result of 2020 Election Using the 2016 Election Data as Training Data.

Next, we attempt to visualize transferable states, conducting a statistical analysis of the results after multiple repetitions. For a swing state, we record the frequency of occurrences for all transferable states and depict states with more than 50% occurrences on the map in green color. As observed in Figure 3, some transferable states exhibit geographical information signals. However, for some targets, the spatial or geographical correlations may not be readily apparent. This is a commonplace occurrence. With the development of the economy, culture, and scientific technology, regional interconnections are no longer confined solely to spatial proximity. Latent economic and political affiliations become pivotal factors.
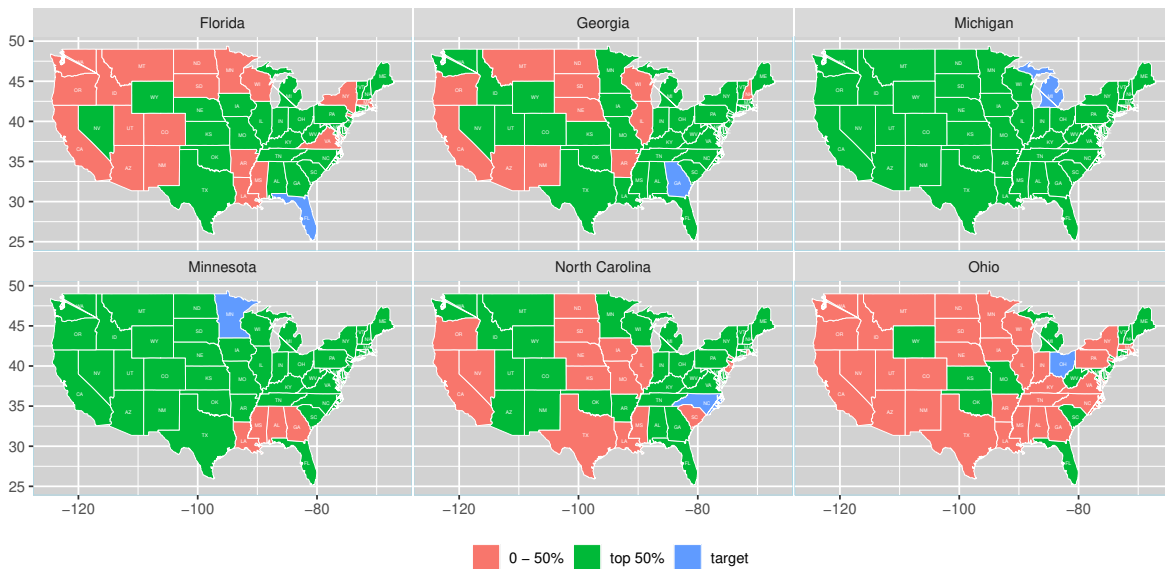
Figure 3: The Detected Transferable States for Each Swing State.

In addition, to provide a comprehensive demonstration of the superiority of the proposed TranSAR method, we treat each state as the target once a time. Subsequently, we conduct both the tranSAR and SAR procedures, and the outcomes have been summarized in Supplementary Materials. In conclusion, our tranSAR method consistently outperforms the traditional SAR method in the majority of cases, yielding superior prediction results.

Motivated by public interest, we also predict the outcome of the 2024 U.S. presidential election for all states using demographic and geographical data in 2022, based on the trained tranSAR model from the 2020 U.S. polling data along with other demographic and geographical data. We use the 2022 demographic data as covariates to predict county-level support rates. And we use the 2020 total vote counts of county-level as weights to calculate state-level support rates (because in the U.S., the "winner-takes-all" system weights each county by its vote count). We focus on the predictions of election outcomes for eight "swing states" following the rule based on whether there was a change in the supported party over the past three elections. Therefore, we select Arizona, Georgia, Florida, Pennsylvania, Michigan, Wisconsin, Ohio, and Iowa as swing states. For non-swing states, we use the results from their last three presidential elections as the outcome for this election, while for swing states, we use our tranSAR method for prediction. Considering the randomness inherent in the algorithm, we conduct multiple rounds of analysis using our TranSAR procedure. In these analyses, if the Democratic Party receive support in more than half of the iterations, the swing state was classified as supporting the Democratic Party; otherwise, it was classified as supporting the Republican Party. We obtain the supporting party for each state (see Figure 4) and calculate the final support vote counts combined with the electoral votes. The final prediction result shows that the Democratic Party receive 309 electoral votes, exceeding the threshold of 269 votes. Therefore, we predict that the outcome of the 2024 U.S. presidential election will favor the Democratic Party.
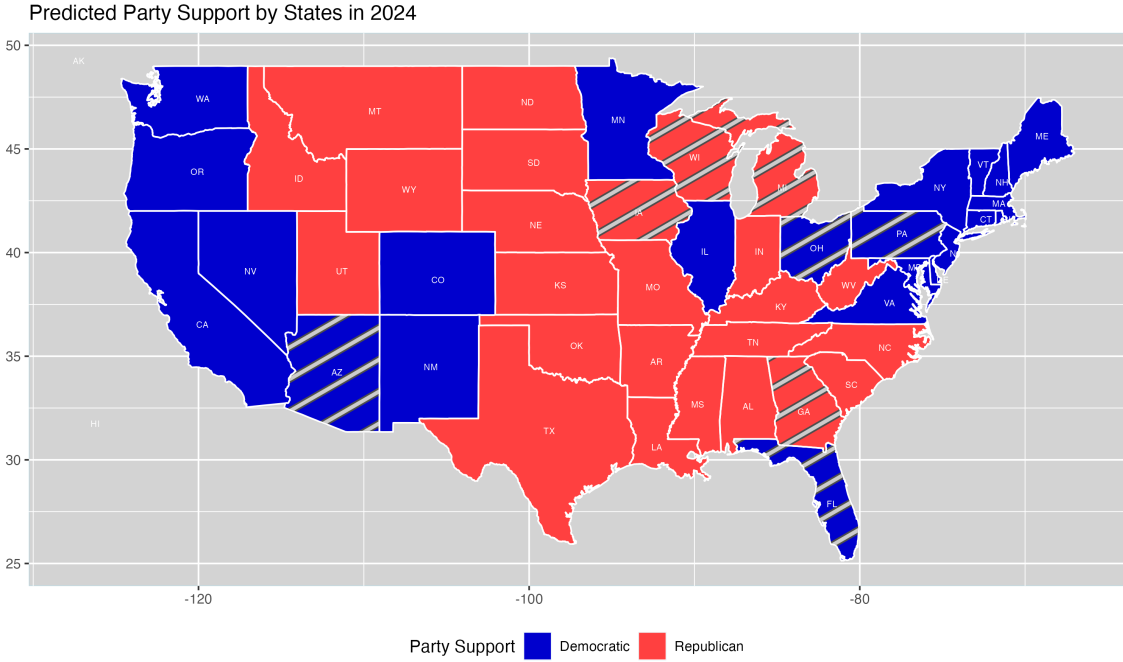
Figure 4: Predicted Party Support by States in 2024. The striped states are the swing states whose election outcomes predicted by our TranSAR method.

6 Theoretical results

In this section, we will establish an estimation convergence rate for the proposed $\mathcal{A}$-*TranSAR* estimator by assuming $\underline{n} \equiv \min_{k \in [K] \cup \{0\}} n_k \to \infty$. Subsection 6.1 is for general results and Subsection 6.2 is based on the 2SLS estimation method. Finally, we prove the consistency of the transferable source detection algorithm in Subsection 6.3.

For theoretical analysis, we define the population form for the above estimator as

$$\omega^{\mathcal{A}} = \underset{\omega \in \mathbb{R}^{p+q}}{\arg \min} \sum_{k \in \mathcal{A}} \alpha_k \bar{\ell}_1^{(k)}(\omega), \tag{16}$$

where $\alpha_k = \frac{n_k}{n_{\mathcal{A}}}$ and $\bar{\ell}_1^{(k)}(\omega)$ is the corresponding population objective function for dataset $\mathfrak{D}^{(k)}$. Under some regularity conditions, the first-stage estimator in Eq. (4) is consistent, i.e., $\hat{\omega} - \omega^{\mathcal{A}} \xrightarrow{p} 0$. Analogously, define the "true parameter" based on the single source k as

$$\omega^{(k)} = \underset{\omega \in \mathbb{R}^{p+q}}{\arg \min} \bar{\ell}_1^{(k)}(\omega). \tag{17}$$

24

6.1 Convergence rate when $\mathcal{A}_h$ is known

Assumption 1 (Network structure)**.** *The spatial weight matrices $W_l^{(k)}(k \in \{0\} \cup [K], l \in [p])$ are non-stochastic with zero diagonals, and p is fixed and does not depend on n_0 or n_k. $S^{(k)}(\lambda) = I_{n_k} - \sum_{l=1}^p \lambda_l^{(k)} W_l^{(k)}$ is invertible for all $\lambda \in \Lambda$, where the parameter space Λ is compact. Matrices $W_l^{(k)}$ and $S^{(k)}(\lambda)^{-1}$ are uniformly bounded in both row and column sum norms for all $n_k, k \in [K] \cup \{0\}, l \in [p]$ and $\lambda \in \Lambda$. And for all large enough n_k, $\|W_l^{(k)} S^{(k)}(\lambda)^{-1}\|_F / \sqrt{n_k}$ is bounded away from zero and infinity uniformly over $k \in [K] \cup \{0\}, l \in [p]$ and $\lambda \in \Lambda$.*

Assumption 2 (Regular conditions for the design matrix and error terms)**.**

(1) *Denote $\mathbf{X}^{(0)} \equiv (\mathbf{x}_1^{(0)}, \ldots \mathbf{x}_{n_0}^{(0)})^\mathsf{T}$ and the covariance matrix of $\mathbf{x}_i^{(0)}$ for each i is Σ_0. For any $\beta \in \mathbb{R}^q, \mathbf{x}_i^{(0)\mathsf{T}} \beta$ $(i \in [n_0])$, are i.i.d. $\kappa_0 \|\beta\|_2$ sub-Gaussian with mean zero, and $0 < \underline{\psi_0} = \lambda_{\min}(\Sigma_0) \le \lambda_{\max}(\Sigma_0) = \overline{\psi_0} < \infty$.*

(2) *The error terms $V_i^{(0)}$ $(i \in [n_0])$ are i.i.d. sub-Gaussian with mean zero and variance σ^2.*

(3) *As $n_0 \to +\infty$, $\mathbb{P}\left(\lambda_{\min}(\frac{(\widehat{\mathbb{X}}^{(0)})^\mathsf{T} \widehat{\mathbb{X}}^{(0)}}{n_0}) \ge \phi_0\right) \to 1$, where ϕ_0 is a positive constant.*

Assumption 3 (Convergence rates of the first step estimator)**.** *The first step estimator $\widehat{\omega}$ minimizing (4) satisfies $\|\widehat{\omega} - \omega^{\mathcal{A}}\|_1 = O_{\mathbb{P}}(a_{n_\mathcal{A}}^{(1)})$, and $n_\mathcal{A}^{-1}\|\mathbb{X}^{\mathcal{A}}(\widehat{\omega} - \omega^{\mathcal{A}})\|_2^2 = O_{\mathbb{P}}(a_{n_\mathcal{A}}^{(2)})$, where $a_{n_\mathcal{A}}^{(1)} \to 0$ and $a_{n_\mathcal{A}}^{(2)} \to 0$ as $n_\mathcal{A} \to \infty$, and $\mathbb{X}^{\mathcal{A}}$ is stack of $\mathbb{X}^{(k)}$ for $k \in \mathcal{A}$.*

Assumption 4 (Instruments)**.** *When n_0 is large enough, the IV matrix*

$$Q^{(0)} = \left(\mathbf{X}^{(0)}, W_1^{(0)}\mathbf{X}^{(0)}, \ldots, W_q^{(0)}\mathbf{X}^{(0)}\right) \tag{18}$$

satisfies $0 < \psi_*^{(0)} \le \frac{1}{\sqrt{n_0}}\|Q^{(0)}\|_2 \le \psi^{(0)*} < \infty$ for some constants $\psi_*^{(0)}$ and $\psi^{(0)*}$. There exist constant coefficient vectors $\pi_j \in \mathbb{R}^d$ for $j \in [p+q]$ such that $\max_{j=1,\ldots,p+q} \|\widehat{\pi}_j - \pi_j\|_2 = O_{\mathbb{P}}(\sqrt{\log(d)/n_0})$ and $\|\pi_j\|_2^2$ is uniformly bounded over j and n_0, where $\widehat{\pi}_j$ $(j \in [p+q])$ are defined in Eq. (7).

Remark 4. Assumption 1 is standard in spatial econometrics. See Kelejian and Prucha (1999), Lee (2004), Lee (2007) and Lee and Yu (2014). Meanwhile, we assume the number of spatial weight matrices p is fixed, as either one or very few spatial weight matrices are often used in most empirical studies. For example, in our empirical application, $p = 1$. Assumption 2 requires the predictors and error terms to be sub-Gaussian, which is standard in the literature of transfer learning, such as Li et al. (2022b) and Tian and Feng (2023). The eigenvalue condition in Assumption 2 (iii) is widely employed in high-dimensional statistical literature or can be derived from various regular conditions (Mendelson et al., 2008; Negahban et al., 2009; Raskutti et al., 2010; van de Geer and Bühlmann, 2009; Loh and Wainwright, 2012). Assumption 3 imposes some conditions on the convergence rate of the first step estimator, which will be verified using a concrete example in Subsection 6.2. Assumption 4 is about the validity of the instrument matrix $Q^{(0)}$ and the refitted value $\widehat{\mathbb{X}}^{(0)}$.

Theorem 1. (Convergence rate of the $\mathcal{A}$-*TranSAR* estimator) Let the parameter space be $\Theta = \Lambda \times \{\beta \mid \|\beta\|_2 < M\}$ for some positive constant M. Under Assumptions 1-4, if the loss function ℓ_1 is twice differentiable, $\sup_{k \in \mathcal{A}} \|\Sigma^{\mathcal{A}^{-1}} \Sigma^{(k)}\|_1 = \check{C} < \infty$, $s\frac{\log q}{n_0} = o(1)$, $q \asymp d$, and $\lambda_\delta \gtrsim \sqrt{\log(q)/n_0}$, where

$$\Sigma^{(k)} \equiv \int_0^1 \frac{\partial^2}{\partial\theta\partial\theta^\mathsf{T}} \bar{\ell}_1^{(k)}(\theta_0 + t(\omega^{(k)} - \theta_0))dt, \ k \in \mathcal{A}, \tag{19}$$

$$\Sigma^{\mathcal{A}} \equiv \sum_{k \in \mathcal{A}} \int_0^1 \alpha_k \frac{\partial^2}{\partial\theta\partial\theta^\mathsf{T}} \bar{\ell}_1^{(k)}(\theta_0 + t(\omega^{\mathcal{A}} - \theta_0))dt, \alpha_k = \frac{n_k}{n_\mathcal{A}}. \tag{20}$$

Denote $S = \text{support}(\theta_0)$ and $s = |S|$. Then

$$\|\widehat{\theta} - \theta_0\|_2^2 = O_\mathbb{P}\left(\left(\sqrt{\frac{\log q}{n_0}}h\right) \wedge \left(s\frac{\log q}{n_0}\right) \wedge h^2 + a_{n_\mathcal{A}}^{(2)}\right). \tag{21}$$

Remark 5. When we consider the case of fixed dimension of covariates q, under some regularity conditions, $a_{n_\mathcal{A}}^{(2)} = \frac{1}{n_\mathcal{A}}$. Then, we could obtain $\|\widehat{\theta} - \theta_0\|_2^2 = O_\mathbb{P}(\min(n_0^{-1}, h^2) + n_\mathcal{A}^{-1})$, which implies that when the sample size $n_\mathcal{A}$ of the informative source data is large enough and h has a suitable

convergence rate, the estimation convergence rate of the $\mathcal{A}$-*TranSAR* estimator is better than that only using the target data.

6.2 Convergence rate under the 2SLS loss

In this section, we verify the requirements in the above theorem for the 2SLS estimation and simplify the convergence rate of the $\mathcal{A}$-*TranSAR* estimator. As in Eq. (8), let $\ell_1(\cdot \mid \omega)$ be the loss function of the 2SLS. To elaborate, let $Y^{\mathcal{A}}$ denote the stack consisting of $Y^{(k)}$ for all $k \in \mathcal{A}$, i.e., $Y^{\mathcal{A}} = (Y^{(k)\mathsf{T}}, k \in \mathcal{A})^{\mathsf{T}}$. $\mathbf{X}^{\mathcal{A}}$ and $\mathbb{X}^{\mathcal{A}}$ are defined similarly. Then the objective function (4) could be rewritten as

$$\frac{1}{2n_{\mathcal{A}}}\|Y^{\mathcal{A}} - \widehat{\mathbb{X}}^{\mathcal{A}}\omega\|_2^2 + \lambda_\omega\|\omega\|_1, \tag{22}$$

where $\widehat{\mathbb{X}}^{(k)}$ is defined similarly as $\widehat{\mathbb{X}}^{(0)}$ in Subsection 3.1, and $\widehat{\mathbb{X}}^{\mathcal{A}}$ is their stack. Here the IV matrices are $Q^{(k)}$ and $Q^{\mathcal{A}}$. We impose several similar conditions on $\mathfrak{D}^{(k)}$ ($k \in \mathcal{A}$) in the following.

Assumption 5. (Regular conditions for design matrices and error terms on the k-th source) *For source $k \in \mathcal{A}$, we have the following assumptions: (i) For the design matrix $\mathbf{X}^{(k)} = (\mathbf{x}_1^{(k)}, \ldots \mathbf{x}_{n_k}^{(k)})^{\mathsf{T}}$ and any $\beta \in \mathbb{R}^q$, $\mathbf{x}_i^{(k)\mathsf{T}}\beta$ ($i \in [n_k]$) are i.i.d.$\kappa_k\|\beta\|_2$ sub-Gaussian with mean zero for certain constant κ_k, where $\max_{k \in \mathcal{A}} \kappa_k < \infty$. (ii) The error terms $V_i^{(k)}$ ($i \in [n_k]$) are i.i.d. sub-Gaussian with mean zero and variance σ_k^2. (iii) As $n_k \to +\infty$, $\mathbb{P}\left(\lambda_{\min}\left(\frac{\widehat{\mathbb{X}}^{(k)\mathsf{T}}\widehat{\mathbb{X}}^{(k)}}{n_k}\right) \geq \phi_k\right) \to 1$, where ϕ_k is a positive constant.*

Assumption 6 (Instruments for the k-th source)**.** *For the instruments*

$$Q^{(k)} = \left(\mathbf{X}^{(k)}, W_1^{(k)}\mathbf{X}^{(k)}, \ldots, W_q^{(k)}\mathbf{X}^{(k)}\right), \ k \in \mathcal{A} \cup \{0\}, \tag{23}$$

when n_k, the number of rows of $Q^{(k)}$, is large enough, $0 < \psi_*^{(k)} \leq \frac{1}{\sqrt{n_k}}\|Q^{(k)}\|_2 \leq \psi^{(k)*} < \infty$ for some constants $\psi_*^{(k)}$ and $\psi^{(k)*}$. There exist constant coefficient vectors $\pi_j^{(k)} \in \mathbb{R}^d$ for $j \in [p+q]$ such that $\max_{j=1,\ldots,p+q}\|\hat{\pi}_j - \pi_j^{(k)}\|_2 = O_{\mathbb{P}}(\sqrt{\log(d)/n_k})$ and $\|\pi_j^{(k)}\|_2$ is uniformly bounded over j and k.

Under Assumptions 5 and 6, the convergence rate of the $\mathcal{A}$-*TranSAR* estimator is summarized in the following Theorem 2.

Theorem 2. If Assumptions 1, 2, 4, 5, and 6 hold, $\sup_{n_k} \mathbf{B}^{(k)} < \infty$ with $\mathbf{B}^{(k)} \equiv 1 \vee \|\beta_0^{(k)}\|_2$, K is a fixed, $q \asymp d$, $s\frac{\log q}{n_0} = o(1)$, $s^2\frac{\log n_0}{n_0} = o(1)$, $n_{\mathcal{A}} > n_0$, $q^2 h = O(1)$, $\lambda_\delta \gtrsim \sqrt{(\log q)/n_0}$ and $\lambda_\omega \gtrsim \sqrt{(\log q)/n_{\mathcal{A}}}$, where $S = \text{support}(\theta_0)$ and $s = |S|$, then we have

$$\|\widehat{\theta} - \theta_0\|_2^2 = O_{\mathbb{P}}\left((\sqrt{\frac{\log q}{n_0}}h) \wedge (\frac{s\log q}{n_0}) \wedge h^2 + (\frac{\log n_A}{n_A}h^2) \wedge \frac{\log^3 n_A}{n_{\mathcal{A}}^3} + \frac{s\log q}{n_{\mathcal{A}}} \right). \quad (24)$$

Theorem 2 indicates that if $h \ll s\sqrt{\log q/n_0}$ and $n_{\mathcal{A}} \gg n_0$, the $\mathcal{A}$-*TranSAR* estimator is better than the classical 2SLS estimator based on only the target data, which demonstrates the usefulness of transfer learning in the SAR models.

6.3 Detection consistency

Finally, we will show that our proposed transferable source detection algorithm is consistent even for a high dimensional model, i.e., $q \gg n_0$.

Assumption 7 (Identifiability condition)**.** *The tolerance level $h = o(1)$ as the minimal sample size $\underline{n} \equiv \min_{k \in [K] \cup \{0\}} n_k \to \infty$. For any $k \in [K] \cup \{0\}$ and $r \in [3]$, $q\log(q)\|\widetilde{\theta}^{(k)} - \widehat{\theta}^{(k,r)}\|_1 = o_{\mathbb{P}}(1)$. For $k \in \mathcal{A}^c \equiv [K] - \mathcal{A}$, we control the signal power as*

$$\underline{\lambda}\|\theta_0 - \widetilde{\theta}^{(k)}\|_2^2 \geq \|\theta_0 - \widetilde{\theta}^{(k)}\|_1 + \bar{C}\left[(\|\theta_0 - \widehat{\theta}^{(0,r)}\|_1) \vee 1\right] -$$
$$\frac{\sigma^2}{2n_0}\text{tr}\{[(S(\tilde{\lambda}^{(k)}) - S)S^{-1}]^{\mathsf{T}}[(S(\tilde{\lambda}^{(k)}) + S)S^{-1}]\}, \quad (25)$$

and the gap between θ_0 and $\widetilde{\theta}^{(k)}$,

$$\varphi_k \equiv \sqrt{\frac{1}{n_0}}(\|\theta_0 - \widetilde{\theta}^{(k)}\|_1 + 1)^2 = o(1), \quad (26)$$

where $\bar{C} > 0$ is a constant and $\underline{\lambda} \equiv \liminf_{n_0 \to \infty} \lambda_{\min}(\frac{1}{2n_0}\mathbb{E}\mathbf{X}^{\star\mathsf{T}}\mathbf{X}^\star) > 0$, with $\mathbf{X}^\star \equiv (\mathbf{W}^{(0)}(\mathbf{I}_p \otimes (S^{-1}\mathbf{X}^{(0)}\beta_0)), \mathbf{X}^{(0)})$.

Remark 6. Conditions (25) and (26) guarantee a suitable gap between the population-level coefficients in set $\mathcal{A}^c$ and the true coefficient of the target model. Intuitively, assuming an appropriate signal strength is necessary to ensure the consistency of estimators. On the one hand, a very weak signal makes it challenging for the algorithm to differentiate informative and uninformative sources. On the other hand, an excessively strong signal can lead the first step estimator to mimic the model structure of the source, thereby hindering accurate identification.

Next, we establish the detection consistency of $\widehat{\mathcal{A}}$ in the following theorem.

Theorem 3 (Detection consistency of $\widehat{\mathcal{A}}$). If Assumptions (1)-(4) and (7) are satisfied, $\|\beta_0\|_2 < \infty$ and $\frac{\log q}{n_0} = o(1)$, then the automatically detected transferable index set $\widehat{\mathcal{A}}$ in Eq. (14) is consistent, i.e.,

$$\mathbb{P}(\widehat{\mathcal{A}} = \mathcal{A}) \to 1, \text{ as } \underline{n} \to \infty. \tag{27}$$

7 Conclusion

To more accurately explore the spatial factors influencing swing states, we propose a method to enhance the estimation of spatial model in swing states by transferring knowledge from other states. We introduce a transfer learning method within the framework of SAR models, aimed at addressing spatially dependent data of small sample size. The empirical application of this methodology, specifically in predicting U.S. election results in swing states using demographic and geographical data, demonstrates its potential to enhance traditional spatial methods. Based on our comprehensive analysis and the application of the tranSAR model, our prediction for the 2024 U.S. presidential election is a victory for the **Democratic** party. Future research could focus on developing tests to detect informative sets and improving the accuracy of coefficient estimation within the transfer learning framework.

Supplementary Materials

All technical proofs of theorems and the additional simulations are included in the online supplementary materials.

Funding

References

Anselin, L. (1988). *Spatial Econometrics: Methods and Models*, volume 4 of *Studies in Operational Regional Science*. Springer Science & Business Media, Dordrecht.

Baltagi, B. H. and Li, D. (2004). Prediction in the panel data model with spatial correlation. In Anselin, L., Florax, R. J. G. M., and Rey, S. J., editors, *Advances in Spatial Econometrics: Methodology, Tools and Applications*, Advances in Spatial Science, pages 283–295. Springer, Berlin, Heidelberg.

Bastani, H. (2021). Predicting with proxies: Transfer learning in high dimension. *Management Science*, 67(5):2964–2984.

Belloni, A., Chen, D., Chernozhukov, V., and Hansen, C. (2012). Sparse Models and Methods for Optimal Instruments With an Application to Eminent Domain. *Econometrica*, 80(6):2369–2429.

Cai, C., Cai, T. T., and Li, H. (2024a). Transfer learning for contextual multi-armed bandits. *The Annals of Statistics*, 52(1):207–232.

Cai, T. T., Kim, D., and Pu, H. (2024b). Transfer learning for functional mean estimation: Phase transition and adaptive algorithms. *The Annals of Statistics*, 52(2):654–678.

Cai, T. T. and Pu, H. (2019). Transfer learning for nonparametric regression: Non-asymptotic minimax analysis and adaptive procedure.

Case, A., Rosen, H., and Hines, J. (1993). Budget spillovers and fiscal policy interdependence: Evidence from the states. *Journal of Public Economics*, 52(3):285–307.

Cheng, X. and Liao, Z. (2015). Select the valid and relevant moments: An information-based LASSO for GMM with many moments. *Journal of Econometrics*, 186(2):443–464.

Cliff, A. D. and Ord, J. K. (1973). *Spatial Autocorrelation*. Pion, London.

Cliff, A. D. and Ord, J. K. (1975). Model building and the analysis of spatial pattern in human geography. *Journal of the Royal Statistical Society: Series B (Methodological)*, 37(3):297–328.

Fan, J. and Li, R. (2001). Variable selection via nonconcave penalized likelihood and its oracle properties. *Journal of the American Statistical Association*, 96(456):1348–1360.

Fan, J. and Liao, Y. (2014). Endogeneity in high dimensions. *The Annals of Statistics*, 42(3):872–917.

Fotheringham, A. S., Li, Z., and Wolf, L. J. (2021). Scale, context, and heterogeneity: A spatial analytical perspective on the 2016 U.S. presidential election. *Annals of the American Association of Geographers*, 111(6):1602–1621.

Gold, D., Lederer, J., and Tao, J. (2020). Inference for high-dimensional instrumental variables regression. *Journal of Econometrics*, 217(1):79–111.

Grennan, J. (2019). Dividend payments as a response to peer influence. *Journal of Financial Economics*, 131(3):549–570.

Higgins, A. and Martellosio, F. (2023). Shrinkage estimation of network spillovers with factor structured errors. *Journal of Econometrics*, 233(1):66–87.

Hu, X. and Zhang, X. (2023). Optimal parameter-transfer learning by semiparametric model averaging. *Journal of Machine Learning Research*, 24(358):1–53.

Kelejian, H. H. and Prucha, I. R. (1998). A generalized spatial two-stage least squares procedure for estimating a spatial autoregressive model with autoregressive disturbances. *The Journal of Real Estate Finance and Economics*, 17(1):99–121.

Kelejian, H. H. and Prucha, I. R. (1999). A generalized moments estimator for the autoregressive parameter in a spatial model. *International Economic Review*, 40(2):509–533.

Kim, J., Elliott, E., and Wang, D.-M. (2003). A spatial analysis of county-level outcomes in US Presidential elections: 1988–2000. *Electoral Studies*, 22(4):741–761.

Kostov, P. (2009). A spatial quantile regression hedonic model of agricultural land prices. *Spatial Economic Analysis*, 4(1):53–72.

Lee, L.-f. (2003). Best spatial two-stage least squares estimators for a spatial autoregressive model with autoregressive disturbances. *Econometric Reviews*, 22(4):307–335.

Lee, L.-f. (2004). Asymptotic distributions of quasi-maximum likelihood estimators for spatial autoregressive models. *Econometrica*, 72(6):1899–1925.

Lee, L.-f. (2007). GMM and 2SLS estimation of mixed regressive, spatial autoregressive models. *Journal of Econometrics*, 137(2):489–514.

Lee, L.-f. and Yu, J. (2014). Efficient GMM estimation of spatial dynamic panel data models with fixed effects. *Journal of Econometrics*, 180(2):174–197.

Li, S., Cai, T., and Duan, R. (2021). Targeting underrepresented populations in precision medicine: A federated transfer learning approach.

Li, S., Cai, T. T., and Li, H. (2022a). Estimation and inference with proxy data and its genetic applications.

Li, S., Cai, T. T., and Li, H. (2022b). Transfer learning for high-dimensional linear regression: Prediction, estimation and minimax optimality. *Journal of the Royal Statistical Society: Series B (Statistical Methodology)*, 84(1):149–173.

Li, S., Cai, T. T., and Li, H. (2022c). Transfer Learning in Large-Scale Gaussian Graphical Models with False Discovery Rate Control. *Journal of the American Statistical Association*, 118(543):2171–2183.

Liu, X. and Lee, L.-f. (2010). GMM estimation of social interaction models with centrality. *Journal of Econometrics*, 159(1):99–115.

Loh, P.-L. and Wainwright, M. J. (2012). High-dimensional regression with noisy and missing data: Provable guarantees with nonconvexity. *The Annals of Statistics*, 40(3):1637–1664.

Magog the Ogre (2020). English: Results by county of the 2020 United States presidential election.

Mendelson, S., Pajor, A., and Tomczak-Jaegermann, N. (2008). Uniform uncertainty principle for bernoulli and subgaussian ensembles. *Constructive Approximation*, 28(3):277–289.

Negahban, S., Yu, B., Wainwright, M. J., and Ravikumar, P. (2009). A unified framework for high-dimensional analysis of M-estimators with decomposable regularizers. In Bengio, Y., Schuurmans, D., Lafferty, J., Williams, C., and Culotta, A., editors, *Advances in Neural Information Processing Systems*, volume 22. Curran Associates, Inc.

Okunlola, O. A., Alobid, M., Olubusoye, O. E., Ayinde, K., Lukman, A. F., and Szucs, I. (2021). Spatial regression and geostatistics discourse with empirical application to precipitation data in Nigeria. *Scientific Reports*, 11(1):16848.

Ord, J. K. (1975). Estimation methods for models of spatial interaction. *Journal of the American Statistical Association*, 70(349):120–126.

Pan, S. J. and Yang, Q. (2009). A survey on transfer learning. *IEEE Transactions on knowledge and data engineering*, 22(10):1345–1359.

Peters, A., DeYoung, T., and Ross, E. (2004). GIS for get-out-the-vote campaigns using spatial tools, local governments can locate underrepresented communities to improve voter outreach and registration efforts. *Geospatial solutions*, 14:42–57.

Pirinsky, C. and Wang, Q. (2006). Does corporate headquarters location matter for stock returns? *The Journal of Finance*, page 25.

Raskutti, G., Wainwright, M. J., and Yu, B. (2010). Restricted eigenvalue properties for correlated gaussian designs. *Journal of Machine Learning Research*, 11:2241–2259.

Su, W., Bogdan, M., and Candès, E. (2017). False discoveries occur early on the lasso path. *Annals of Statistics*, 45(5):2133–2150.

Tian, Y. and Feng, Y. (2023). Transfer learning under high-dimensional generalized linear models. *Journal of the American Statistical Association*, 118(544):2684–2697.

Tibshirani, R. (1996). Regression shrinkage and selection via the lasso. *Journal of the Royal Statistical Society: Series B (Methodological)*, 58(1):267–288.

Torrey, L. and Shavlik, J. (2010). Transfer learning. In *Handbook of Research on Machine Learning Applications and Trends: Algorithms, Methods, and Techniques*, pages 242–264. IGI global, hershey edition.

van de Geer, S. A. and Bühlmann, P. (2009). On the conditions used to prove oracle results for the Lasso. *Electronic Journal of Statistics*, 3(none).

Ver Hoef, J. M., Peterson, E. E., Hooten, M. B., Hanks, E. M., and Fortin, M.-J. (2018). Spatial autoregressive models for statistical inference from ecological data. *Ecological Monographs*, 88(1):36–59.

Wang, S., Nan, B., Rosset, S., and Zhu, J. (2011). Random lasso. *The Annals of Applied Statistics*, 5(1).

Zhang, C. H. (2010). Nearly unbiased variable selection under minimax concave penalty. *The Annals of Statistics*, 38(2):894–942.

Zhang, X. and Yu, J. (2018). Spatial weights matrix selection and model averaging for spatial autoregressive models. *Journal of Econometrics*, 203(1):1–18.

Zhu, Y. (2018). Sparse linear models and l1-regularized 2SLS with high-dimensional endogenous regressors and instruments. *Journal of Econometrics*, 202(2):196–213.

Zhuang, F., Qi, Z., Duan, K., Xi, D., Zhu, Y., Zhu, H., Xiong, H., and He, Q. (2021). A comprehensive survey on transfer learning. *Proceedings of the IEEE*, 109(1):43–76.